Supplementary information

A two-step high-throughput screening platform for engineering enzymes to cure unsaturated polyester resins

*Christoph Janknecht[1], Francisca Contreras[1], Thomke Belthle[1], Maximilian Nöth[1], Lukas Kalinka[1], Tina Radespiel[2], Ulrich Schwaneberg[1, *]*

[1]Institute of Biotechnology, RWTH Aachen University, Worringerweg 3, 52074 Aachen, Germany

[2]BYK-Chemie GmbH, Abelstraße 45, 46483 Wesel

*Corresponding author, u.schwaneberg@biotec.rwth-aachen.de, +49-241-80-24170, Institute of Biotechnology, RWTH Aachen University, Worringerweg 3, 52074 Aachen, Germany

TABLE OF CONTENT

SUPPLEMENTARY FIGURES AND TABLES

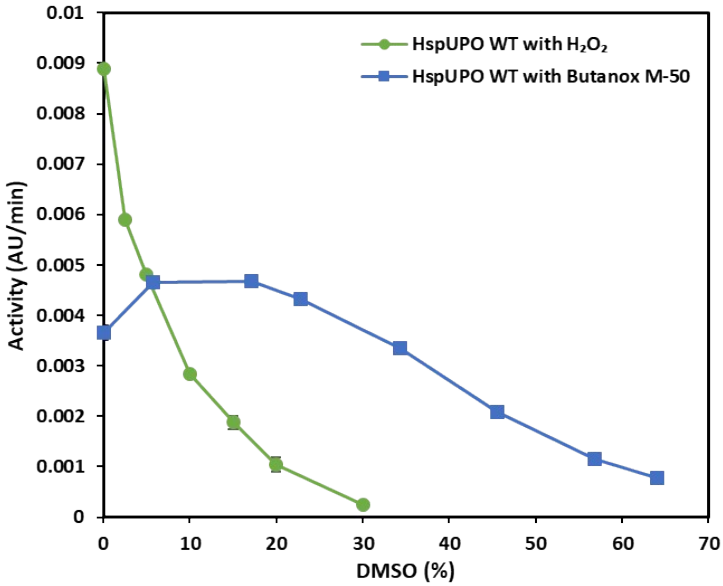

Fig. S1. *Hsp*UPO dimethyl sulfoxide (DMSO) tolerance profile with different peroxides. Activity was measured via the 4-AAP assay with hydrogen peroxide (H_2O_2, 0.6 mM) or Butanox® M-50 (Methyl ethyl ketone peroxide, 0.023 vol%) as the oxidant substrate. Displayed is the DMSO concentration (vol%) in the enzyme sample;100 µl enzyme sample was mixed with 100 µl assay solution after 1 h incubation at room temperature. Activity was measured by capturing the increase of absorbance units (AU) at 480 nm over 10 min. Measurements were performed in triplicate; error bars indicate the standard error of the mean (SEM).

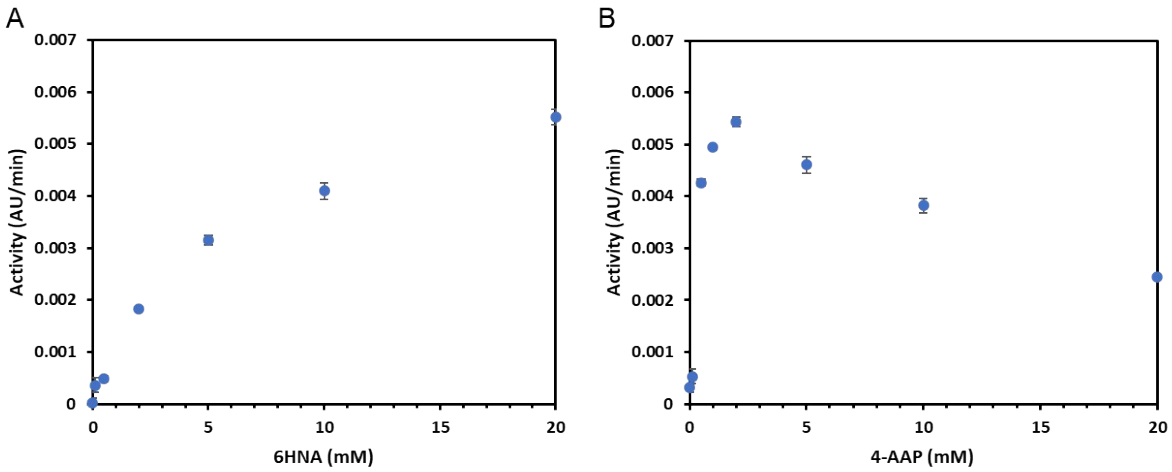

Fig. S2. Optimisation of 4-AAP assay components. (A) 6-hydroxy-2-naphthoic acid (6HNA) was varied to identify the optimal concentration; 2 mM 4-aminoantipyrine (4-AAP). (B) 4-AAP was varied to identify the optimal concentration; 20 mM 6HNA. Displayed is the concentration in the 4-AAP assay solution; 100 µl enzyme sample was mixed with 100 µl assay solution for activity measurements. Activity was measured by capturing the increase of absorbance units (AU) at 480 nm over 10 min. Measurements were performed in triplicate; error bars indicate the standard error of the mean (SEM).

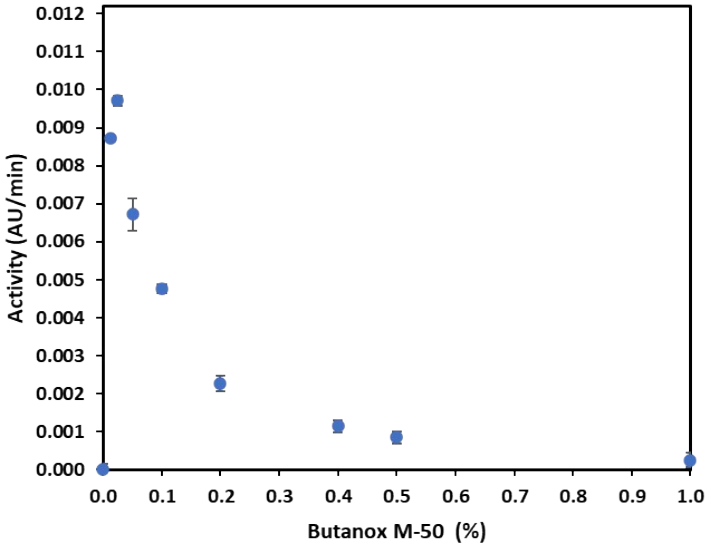

Fig. S3. Influence of Butanox® M-50 (Methyl ethyl ketone peroxide) concentration on *Hsp*UPO activity in the 4-AAP assay. Displayed is the concentration (vol%) in the 4-AAP assay solution; 100 µl enzyme sample was mixed with 100 µl assay solution for activity measurements. Activity was measured by capturing the increase of absorbance units (AU) at 480 nm over 10 min. Measurements were performed in triplicate; error bars indicate the standard error of the mean (SEM).

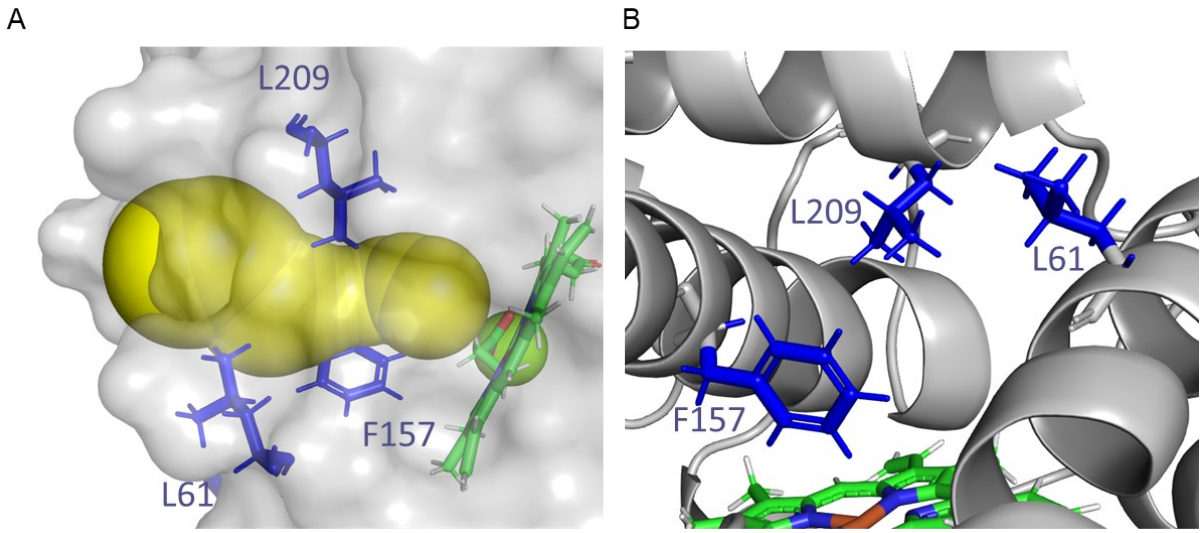

Fig. S4. Structural context of residues selected for site-saturation mutagenesis in HspUPO. (A) Surface representation showing the substrate access tunnel (yellow) and the positions of residues L61, F157, and L209 (blue) lining the tunnel wall as identified by CAVER analysis. (B) Cartoon representation highlighting that the selected residues are located on three distinct α-helices forming the substrate tunnel, illustrating the structure-guided selection of representative tunnel positions.

Table S1: Residues lining the substrate tunnel of *Hsp*UPO identified by CAVER analysis. Axial positions refer to the distance along the tunnel centerline starting from the heme cofactor. Minimum distances were calculated between residue atoms and the tunnel centerline. Selected residues for site-saturation mutagenesis are highlighted in grey.

Residue		Axial position (Å)	Min. distance to centerline (Å)	Contribution to tunnel geometry
161	**GLU**	0.00	3.13	sidechain
162	**SER**	0.00	8.20	backbone
165	**TYR**	0.48	7.34	backbone
164	**ALA**	0.92	3.38	backbone
168	**ALA**	1.29	5.63	sidechain
163	**ILE**	2.92	7.15	sidechain
160	**GLY**	3.27	4.18	backbone (Gly)
159	**LEU**	5.03	7.82	sidechain
209	**LEU**	5.53	4.22	sidechain
58	**LEU**	6.53	6.25	sidechain
157	**PHE**	6.53	4.18	sidechain
153	**LEU**	7.91	6.25	sidechain
156	**ALA**	7.91	5.10	sidechain
65	**PHE**	8.30	5.00	sidechain
61	**LEU**	8.63	5.03	sidechain
206	**THR**	10.12	5.85	sidechain
210	**GLY**	10.12	5.84	backbone (Gly)
213	**SER**	10.12	5.90	sidechain
232	**ARG**	10.57	5.47	sidechain

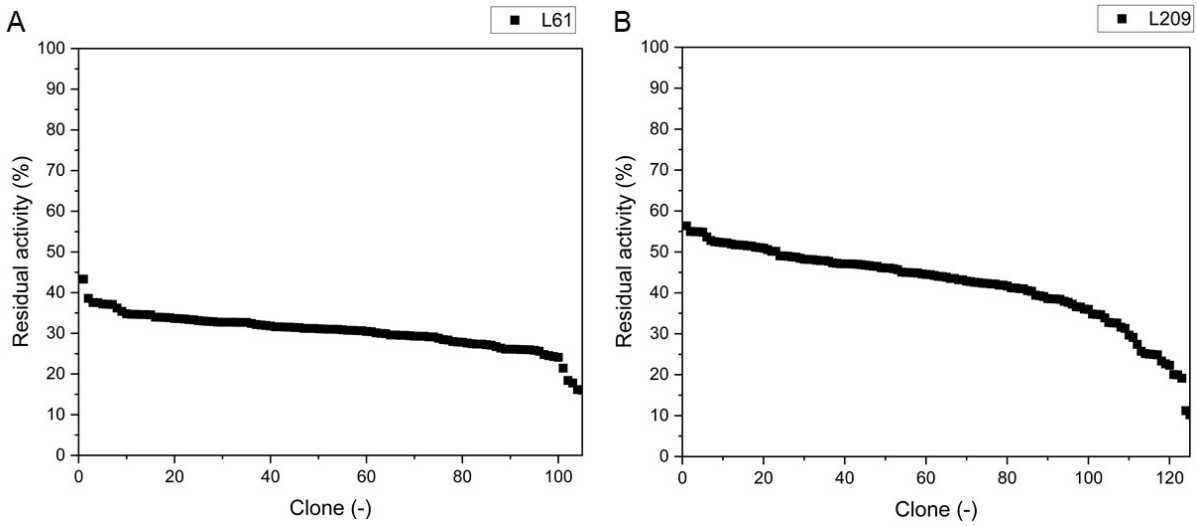

Fig. S5. Screening landscapes of the Site-Saturation Mutagenesis library screening at *Hsp*UPO postions L61 and L209. Results of residual activity of *Hsp*UPO L61 (A) and L209 (B) Site-Saturation Mutagenesis library. Residual activity was calculated from 4-AAP assay activity measurements before and after 1 h incubation in 45 vol% DMSO. 176 variants were screened in total; shown are only variants with measurable initial activity.

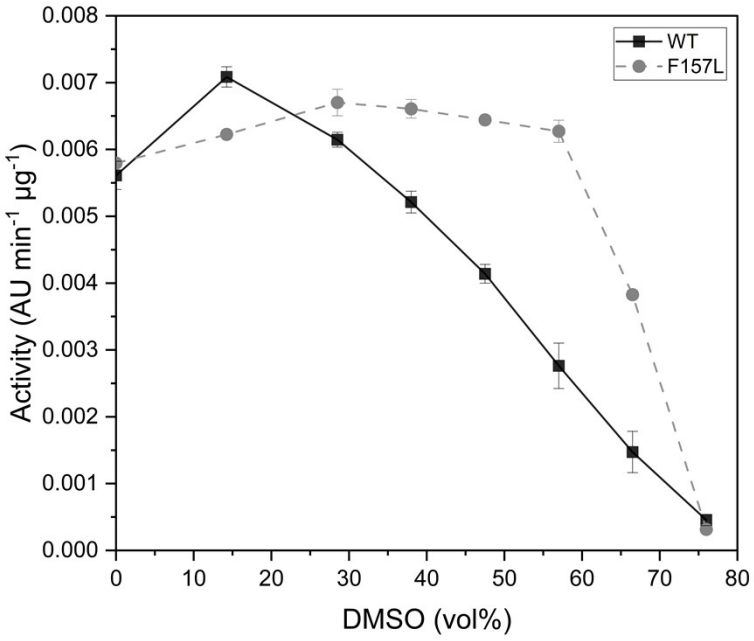

Fig. S6: Absolute activity of *Hsp*UPO WT and variant F157L in different DMSO concentrations. Absolute enzyme activities (AU min^{-1} μg^{-1}) of purified *Hsp*UPO WT (solid line) and the variant F157L (dashed line) were determined via the 4-AAP assay after 1 h incubation in varying concentrations (vol%) of DMSO. Activity was measured by capturing the increase of absorbance units (AU) at 480 nm over 10 min. Measurements were performed in at least duplicates; error bars indicate the standard error of the mean (SEM).

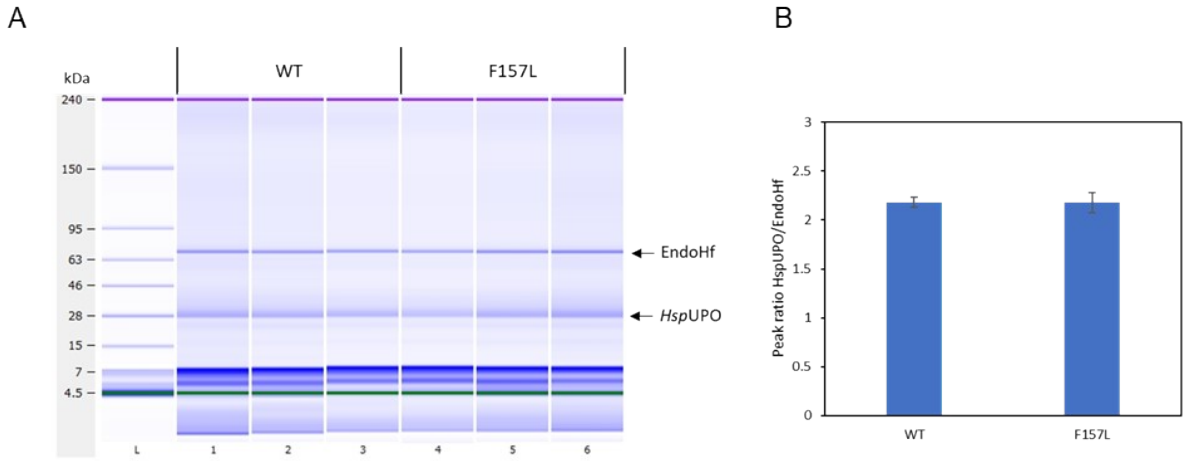

Fig. S7. Determination of *Hsp*UPO content in concentrated *P. Pastoris* supernatant via automated electrophoresis. (A) 2100 Bioanalyzer gel image of *Hsp*UPO WT and F157L. (B) Peak area ratio of *Hsp*UPO band and EndoHf band. Supernatant of *Hsp*UPO WT and variant F157L (200 mL) was concentrated to 1 mL and deglycosylated (28 kDa) with 15 U EndoHf (1 h, 37°C). Peak areas of *Hsp*UPO (28 kDa) and EndoHf (70 kDa, 215 µg mL^{-1}) were calculated and samples were normalised by dilution (600 µL final volume) prior to lyophilisation. Measurements were performed in triplicate; error bars indicate the standard error of the mean (SEM).

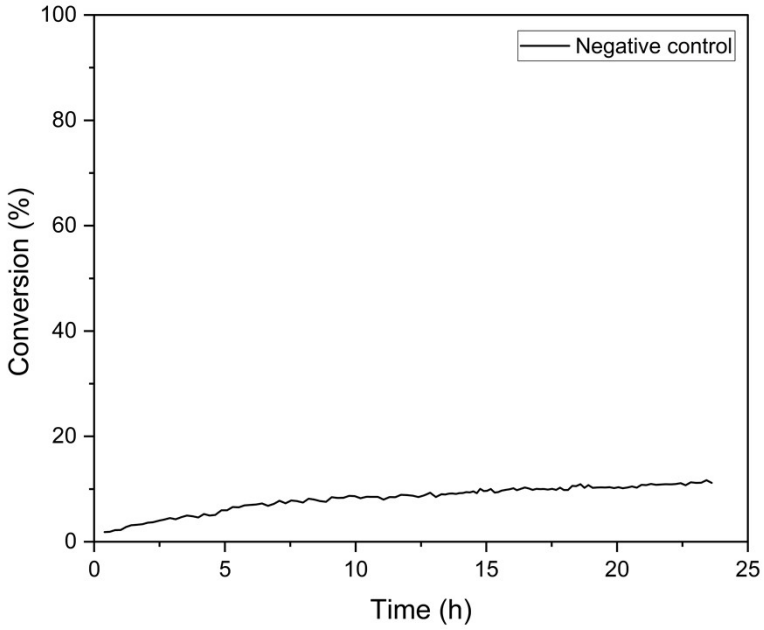

Fig. S8: Raman-based curing measurement of an unsaturated polyester resin in the presence of DMSO mediator without enzyme addition (negative control). Data were acquired under identical conditions as enzymatic curing experiments. Shown is the average of three individual measurments.

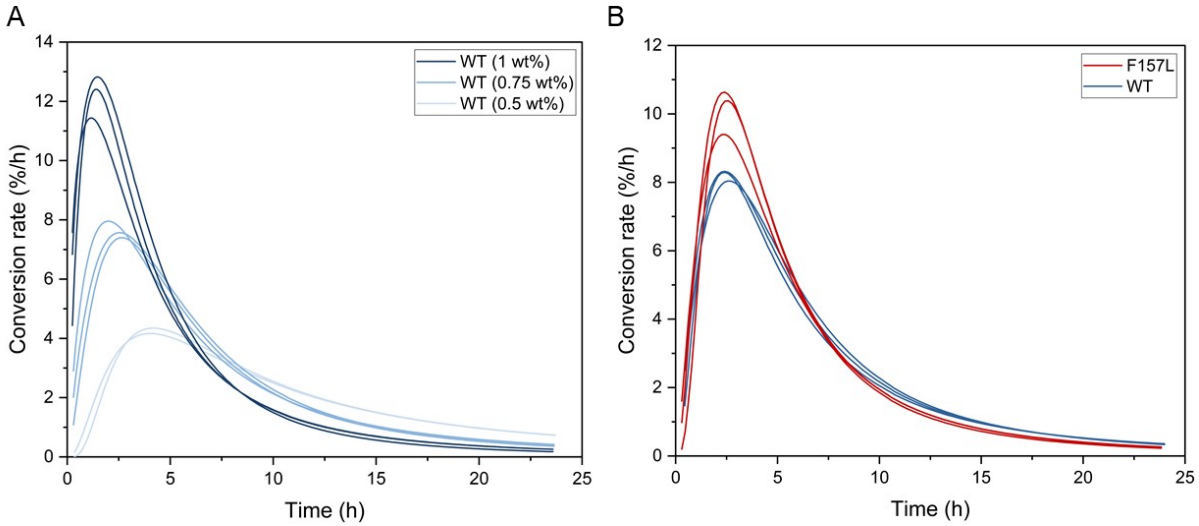

Fig. S9. Conversion rates of *Hsp*UPO-initiated unsaturated polyester resin curing. (A) Conversion rates of three different concentrations (wt%) of *Hsp*UPO WT. (B) Conversion rates of HspUPO WT and F157L (0.75 wt%). Raman conversion data was fitted to a logistic function and conversion rates were determined from its derivative. Measurements were performed in at least duplicates.

Table S2. Nucleotide and amino acid sequences of *Hsp*UPO WT and variant F157L.

Name	Nucleotide Sequence	Amino Acid Sequence
***Hsp*UPO WT**	atgagattcccatctattttcaccgctgtcttgttcgctgcctcctctg cattggctgcccctgttaacactaccactgaagacgagactgctca aattccagctgaagcagttatcggttactctgaccttgagggtgatt tcgacgtcgctgttttgccttttctctgcttccattgctgctaaggaag agggtgtctctctcgagaagagagaggccgaagct[x]gctccttccc cttcttctggttggcaggctcctggtccaaacgatgtccgtgcacct tgtcctatgctgaacactttagccaatcacggtttcctgccacacga tggtaaaggtatcactgtgaacaaaaccattgacgctttgggttca gccttgaacattgacgccaacttgtctacccttttgttcggtttcgct gcaactaccaaccctcaaccaaacgctactttcttcgatcttgacc atctttctcgtcacaacatcctggagcacgatgcctcattgtcaaga caggattcatacttcggtcctgctgatgtgttcaacgaagccgtttt caaccaaaccaagtccttctggactggtgacatcatcgatgttcag atggctgccaacgctagaatcgttagacttcttacttccaacttgac taacccagagtactctttgtctgacctgggatctgctttctctatcgg tgaatcagcagcttacatcggtatcttgggagataagaaatctgca actgtcccaaagtcctgggttgagtatcttttcgaaaacgaaagat tgccatacgagttgggattcaagcgtcctaacgacccattcactac tgacgacttgggagatctgtccactcagatcatcaacgctcaacac tttccacagtctcctggtaaggttgaaaagcgtggtgatactcgttg tccatacggttaccactaataa	MRFPSIFTAVLFAASSALA[x]APVN TTTEDETAQIPAEAVIGYSDLEGD FDVAVLPFSASIAAKEEGVSLEKR EAEAAPSPSSGWQAPGPNDVR APCPMLNTLANHGFLPHDGKGI TVNKTIDALGSALNIDANLSTLLF GFAATTNPQPNATFFDLDHLSR HNILEHDASLSRQDSYFGPADVF NEAVFNQTKSFWTGDIIDVQMA ANARIVRLLTSNLTNPEYSLSDLG SAFSIGESAAYIGILGDKKSATVPK SWVEYLFENERLPYELGFKRPND PFTTDDLGDLSTQIINAQHFPQS PGKVEKRGDTRCPYGYH**
***Hsp*UPO F157L**	atgagattcccatctattttcaccgctgtcttgttcgctgcctcctctg cattggctgcccctgttaacactaccactgaagacgagactgctca aattccagctgaagcagttatcggttactctgaccttgagggtgatt tcgacgtcgctgttttgccttttctctgcttccattgctgctaaggaag agggtgtctctctcgagaagagagaggccgaagct[x]gctccttccc cttcttctggttggcaggctcctggtccaaacgatgtccgtgcacct tgtcctatgctgaacactttagccaatcacggtttcctgccacacga tggtaaaggtatcactgtgaacaaaaccattgacgctttgggttca gccttgaacattgacgccaacttgtctacccttttgttcggtttcgct gcaactaccaaccctcaaccaaacgctactttcttcgatcttgacc atctttctcgtcacaacatcctggagcacgatgcctcattgtcaaga caggattcatacttcggtcctgctgatgtgttcaacgaagccgtttt caaccaaaccaagtccttctggactggtgacatcatcgatgttcag atggctgccaacgctagaatcgttagacttcttacttccaacttgac taacccagagtactctttgtctgacctgggatctgct**ttg**tctatcgg tgaatcagcagcttacatcggtatcttgggagataagaaatctgca actgtcccaaagtcctgggttgagtatcttttcgaaaacgaaagat tgccatacgagttgggattcaagcgtcctaacgacccattcactac tgacgacttgggagatctgtccactcagatcatcaacgctcaacac tttccacagtctcctggtaaggttgaaaagcgtggtgatactcgttg tccatacggttaccactaataa	MRFPSIFTAVLFAASSALA[x]APVN TTTEDETAQIPAEAVIGYSDLEGD FDVAVLPFSASIAAKEEGVSLEKR EAEAAPSPSSGWQAPGPNDVR APCPMLNTLANHGFLPHDGKGI TVNKTIDALGSALNIDANLSTLLF GFAATTNPQPNATFFDLDHLSR HNILEHDASLSRQDSYFGPADVF NEAVFNQTKSFWTGDIIDVQMA ANARIVRLLTSNLTNPEYSLSDLG SA**L**SIGESAAYIGILGDKKSATVPK SWVEYLFENERLPYELGFKRPND PFTTDDLGDLSTQIINAQHFPQS PGKVEKRGDTRCPYGYH**

[x]α-mating signal signal sequence is cleaved off (Numbering starts afterwards).
Substituted codons/amino acids are in bold.

Table S3. Primer sequences for Site-Directed Mutagenesis of *Hsp*UPO L61, F157, and L209.

Primer Name	Sequence
HspUPO_SSM_L61_fwd	cttgtctaccNNKttgttcggtttcgctgcaactac
HspUPO_SSM_L61_rev	aaccgaacaaMNNggtagacaagttggcgtcaatgttc
HspUPO_SSM_F157_fwd	gggatctgctNNKtctatcggtgaatcagcagcttac
HspUPO_SSM_F157_rev	caccgatagaMNNagcagatcccaggtcagacaaag
HspUPO_SSM_L209_fwd	tactgacgacNNKggagatctgtccactcagatcatc
HspUPO_SSM_L209_rev	acagatctccMNNgtcgtcagtagtgaatgggtcgttag
HspUPO_colony_fwd	cacggagtctacatcaagctgt
HspUPO_colony_rev	acccctaccacaagatattcatctg